Synthesis and Characterization of Core-Shell SiO_2 Nanoparticles/Poly(3-aminophenylboronic acid) Composites

Yu-Ping Zhang,[1] Se-Hee Lee,[2,3] Kakarla Raghava Reddy,[2] Anantha Iyengar Gopalan,[2,4] Kwang-Pill Lee[2,3]

[1]*Institute of Applied Chemistry, Henan Institute of Science and Technology, Xinxing 453003, People's Republic of China*
[2]*Department of Chemistry Graduate School, Kyungpook National University, Daegu 702-701, South Korea*
[3]*Nano Practical Application Center, Daegu 704-230, South Korea*
[4]*Department of Industrial Chemistry, Nanomaterials Laboratory, Alagappa University, Karaikudi-630003, India*

Received 26 April 2006; accepted 30 November 2006
DOI 10.1002/app.25938
Published online in Wiley InterScience (www.interscience.wiley.com).

ABSTRACT: SiO_2/Poly(3-aminophenylboronic acid) (PAPBA) composites were synthesized under different experimental conditions, using ultrasonic irradiation method. Polymerization was carried out in the presence of sodium fluoride and D-fructose to anchor 3-aminophenylboronic acid groups on to SiO_2 surface. The SiO_2/PAPBA nanocomposite prepared by NaF and D-fructose in the polymerization medium was found to show different morphology, electrical properties, thermal behavior and structural characterization in comparison to the nanocomposites prepared under other conditions. Ultrasonic irradiation minimizes the aggregation of nanosilica and promotes anchoring of PAPBA units over SiO_2 surface. The morphology of PAPBA/SiO_2 nanocomposite was investigated by using transmission electron microscopy, UV-visible spectroscopy; thermogravimetric analysis, Fourier transform infrared spectroscopy, and X-ray diffraction analysis were used for characterization. Transmission electron microscope of the nanocomposites observation shows that SiO_2/PAPBA composite, prepared with D-fructose and NaF under ultrasonication has a core–shell morphology. The thermal and crystalline properties of core-shell SiO_2/PAPBA nanocomposite was prepared via ultrasonication method is different from the SiO_2/PAPBA nanocomposite prepared via conventional stirring method, in which SiO_2 nanoparticles are submerged in PAPBA. Conductivity of the composite prepared via ultrasonication shows around 0.2 S/cm. J Appl Polym Sci 104: 2743–2750, 2007

Key words: sonochemical synthesis; SiO_2 nanoparticles; poly(aminophenylboronic acid); nanocomposite

INTRODUCTION

Conducting polymer-based nanomaterials have been proved to be suitable for applications in electrical, optical, and sensor devices.[1–5] Various techniques and methods such as nanolithography,[6] the Langmuir–Blodgett technique,[7] chemical or electrochemical polymerization using templates like membrane,[8] porous silica,[9] surfactant aggregates,[10] liquid crystals,[11] and metal nanoparticles as templates[12] etc., have been developed for the preparation of these type of nanomaterials. Further, it is well documented that various conducting polymers and oligomers can self-assemble into supramolecular structures both in solution and at interfaces.[13,14] However, architecturing functional properties in these nanomaterials are still challenging aspect in-depth investigations. Ultrasonic irradiation can be effectively utilized for the preparation of conducting polymers with functional properties.

Ultrasonic irradiation, in the frequency range from 20 kHz to 1 MHz, has been widely used in chemical synthesis as it provides suitable environment and an increased rate for many chemical reactions[15,16] etc. Advantages of using ultrasonication in comparison with other methods for the preparation of nanomaterials include a higher reaction rate, ability to disperse particles, and higher yield of products.[17] Ultrasonic irradiation generates a large number of microbubbles that grow, collapse, and create localized hot spots in a very short time, about a few microseconds. The cavities provide energy to cause chemical and mechanical effects.[16] These conditions have been successfully employed for the preparation of nanoparticles of amorphous metal alloys,[18] carbides,[19] oxides,[20] sulfides,[21] proteinaceous nanospheres,[22] and nanocrystalline materials.[23–25]

Most recently, ultrasonication induced functionalization of carbon nanotubes and formation of nanocomposite with metal nanoparticles have been reported.[26–28] Preparation of Ag_2S/polyvinylalcohol

Correspondence to: K. P. Lee (kplee@knu.ac.kr).
Contract grant sponsor: Korea-China Joint Research Program; contract grant number: F01-2006-000-10,119-0.

(PVA) and CuS/PVA composite have been prepared by ultrasonic irradiation.[29] Wang et al.[30] reported one-dimensional growth of poly(styrene) within the galleries of montmorillonite. Ultrasonicaiton was used to break the aggregates of nanosilica in an aqueous medium to prepare stable poly(*n*-butyl acrylate)/nano-SiO_2 composite.[31] Polyaniline (PANI) and several other polymer based composites have been synthesized by using ultrasound.[32–34] Ultrasonic irradiation has also been utilized for the preparation of nanocomposites of conducting polymers with metal nanoparticles and improved properties of resulting composite material.[35–37]

PANI is unique among conducting polymers as it possesses well-behaved electrochemistry, good environmental stability, and electrochromism.[38] The use of PANI for applications is restricted because of its poor solubility, less thermal stability, loss of conductivity at high temperature, and poor processability both in melt and solution conditions.[39] Substituted PANI with functional groups such as —SO_3H, —COOH or doped with functional protonic acids, such as camphor sulfonic acid, dodecylbenzenesulfonic acids, etc. are having better solubility and processability over PANI.[38,40] However, only limited studies are available on the preparation of PANI derivatives with boronic acid as substituent.[41] It has been shown that polymerization of 3-aminophenylboronic acid (APBA) occurs through a fluoride-catalyzed reactions.[42,43] In an another report,[44] boronate groups were self-assembled on glassy carbon electrode and used for recognizing glycoprotein peroxide. Pristine PANI does not show the electroactivity at neutral and physiological pHs. This restricts the use of PANI for developing biosensors. However, substituted PANI derivatives exhibit characteristics that are suited for biosensor applications. Poly(3-aminophenylboronic acid) (PAPBA) has been used in the detection of fluoride, saccharides, dopamine, and biosensing technology due to high redox activity, conductivity in neutral pH solutions, and switchability between self-doped and nonself-doped states.[45–49] In addition, incorporation of metal nanoparticles into conducting polymers can enhance the conductivity, thermal stability, sensitivity, and selectivity for molecules that are required for a sensor materials.[50,51]

SiO_2 nanoparticles received recent attention because of their superior properties over the microsize particles.[52,53] However, its nanocomposites with organic polymers, SiO_2 generally exists as agglomerates. It becomes important to disperse the SiO_2 particles in the nanocomposites with other polymers for utilizing the synergic properties and fluid applications. Owing to the many uses of silica,[52,53] various polymer–silica composites have been studied. Tang and coworkers[54] reported the phase morphology and particle structure of a poly(ethyl acrylate)–SiO_2 composite. Poly(ethylene-2,6-naphthalate)–SiO_2,[55] polyimide–SiO_2,[56] ethylene–propylene–diene-terpolymer/SiO_2,[57] polypyrrole–SiO_2[58] hybrids etc. have been prepared. Nanocomposites of SiO_2 with conducting polymers are expected to be suitable for applications like sensors, catalysts, etc.

In the present study, nanocomposites of SiO_2 with poly(3-aminophenylboroni acid), PAPBA were prepared under different experimental conditions. Nanocomposites were prepared by the polymerization of aminophenylboronic 3-acid by keeping SiO_2 nanoparticles, D-fructose, and sodium fluoride in the medium. The mixture was subjected to ultrasonication during polymerization. Morphology, electronic properties, thermal behavior of the SiO_2/PAPBA nanocomposites prepared by keeping D-fructose, and NaF in the medium of polymerization were compared with the nanocomposites prepared under other conditions. Further, transmission electron microscopy (TEM), UV-visible spectroscopy, Fourier transform infrared (FTIR) spectroscopy, thermogravimetric analysis, and X-ray diffraction (XRD) analysis were used for the characterization of nanocomposites.

EXPERIMENTAL

Chemicals

Tetraethyl orthosilicate (TEOS) and *m*-APBA were received from Sigma-Aldrich (St. Louis, MO). Ammonium peroxydisulphate, ammonium hydroxide, sodium fluoride, and fructose were used as received (DC chemicals, Seoul, Korea).

Synthesis

Synthesis of SiO_2 nanoparticles

SiO_2 nanoparticles were prepared by mixing TEOS (1.7 mL) with ethanol solution (50 mL) containing ammonium hydroxide (1.5 mL) under vigorous stirring. The mixture was sonicated for 3 h. A white mass was isolated by centrifugation (4000 rpm, 30 min), washed with ethanol and dried under reduced pressure.

Synthesis of SiO_2/PAPBA nanocomposites

A typical procedure for the preparation of SiO_2/PAPBA-NCs is outlined. 0.1 g of SiO_2 nanoparticles was added to an aqueous (18 mL) solution containing 0.372 g of APBA, 0.01 g of NaF, and 0.1 g of D-fructose. The mixture was deoxygenated by passing nitrogen for 10 min. A solution (2 mL) of 0.5*M* ammonium peroxydisulphate was added drop wise and the solution was subjected to sonication for 1 h with a high-intensity ultrasonic probe (Sonics and Materials, VC-600, 20 KHz, Ti horn, 100 W cm^{-2}) at 5°C. A green color so-

lution was obtained. Ethanol was added to the green colored solution and the precipitate (green color) [designated as SiO_2/PAPBA-NC (D-fructose, NaF)] was filtered, washed with ethanol, and dried in vacuum. The nanocomposites were also prepared by adopting a similar procedure but in the absence of NaF and D-fructose in the reaction medium. The SiO_2/PAPBA nanocomposites prepared by keeping D-fructose and NaF in the polymerization under ultrasonication, was designated as SiO_2/P APBA-NC**1**. The SiO_2/PAPBA composites prepared in the absence of NaF and D-fructose under ultrasonication is designated as SiO_2/PAPBA-NC**2**. SiO_2/PAPBA nanocomposite was also prepared via conventional stirring method in the presence of D-fructose and NaF under similar conditions as described procedure for SiO_2/PAPBA-NC1.

Structural characterization

FTIR spectra were recorded on a Bruker IFS 66V FTIR in the region of 400–4000 cm^{-1} using KBr pellets. UV–visible spectra were recorded in DMF by using Beckman UV-visible (DU7500) spectrophotometer. Morphology measurements and particle size determination were made for SiO_2/PAPBA-NCs by using Phillips CM-30 TEM with an accelerating voltage of 100 kV. Thermo gravimetric analysis (TGA) of SiO_2 nanoparticles and SiO_2/PAPBA-NCs was made using a Dupont 9900/2100 TGA at a heating rate of 10°C/min under a nitrogen atmosphere over a temperature range of 30–800°C. XRD patterns of nanocomposites were recorded, using Rigaku Diffractomer with Nickel filtered Cu Kα radiation. Room temperature conductivity was measured on pressed pellets of the composites, using standard four-probe method.

RESULTS AND DISCUSSION

Morphology of SiO_2/PAPBA nanocomposites

Polymerization was performed in the presence ultrasonication for a mixture having 3-amionophenylboronic acid (APBA) and SiO_2 nanoparticles under different experimental conditions. We have selected few experimental conditions for the polymerization that facilitated complexation between aromatic boronic acid groups and SiO_2 nanoparticles. Complexation between the hydroxyl groups in SiO_2 nanoparticle and boronic acid groups in APBA predominantly occurs at neutral medium and influenced by F^- ions.

We have carried out polymerization of APBA in the presence of SiO_2 nanoparticles under ultrasonication, in which medium was maintained with/without using combination of NaF and D-fructose. Morphology of the SiO_2/PAPBA-NCs was found to depend on the conditions used for polymerization. Typically, a careful comparison of TEM images (Fig. 1) reveals a clear difference in morphology was noticed between SiO_2/PAPBA-NC**1** and SiO_2/PAPBA-NC**2**. TEM images (Fig. 1) reveal that SiO_2/PAPBA-NC**1** has a core-shell type morphology, while SiO_2/PAPBA-NC**2** shows the presence of mixture of PAPBA and SiO_2

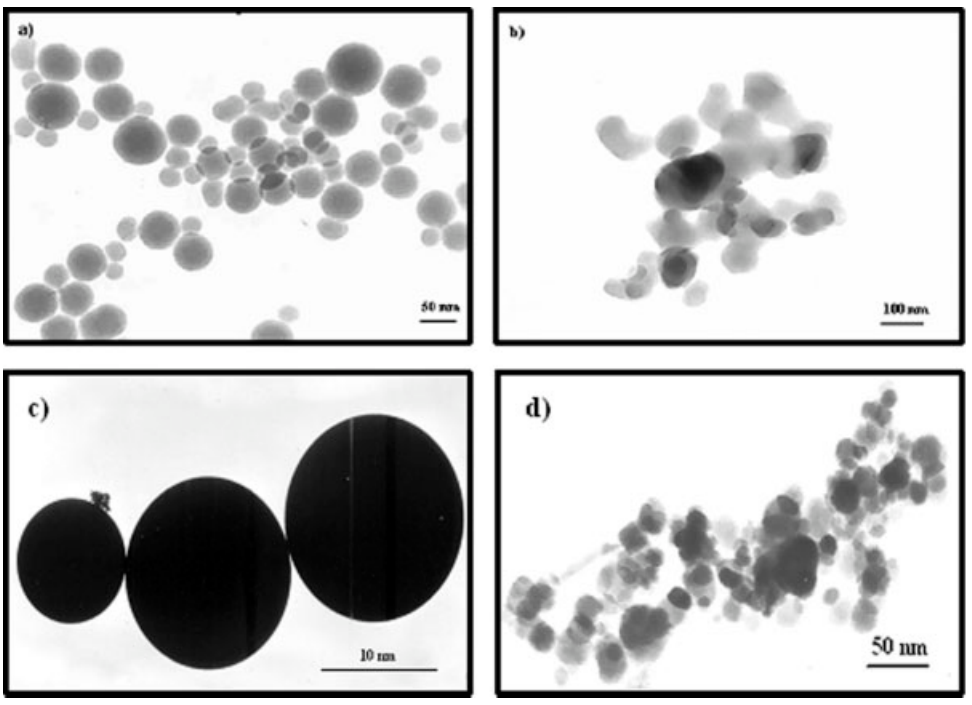

Figure 1 TEM micrographs of (a) SiO_2/PAPBA-NC**1** and (b) SiO_2/PAPBA-NC**2** prepared via ultrasonication, (c) SiO_2 nanoparticles, and (d) SiO_2/PAPBA-NC**1** composite prepared via conventional stirring method.

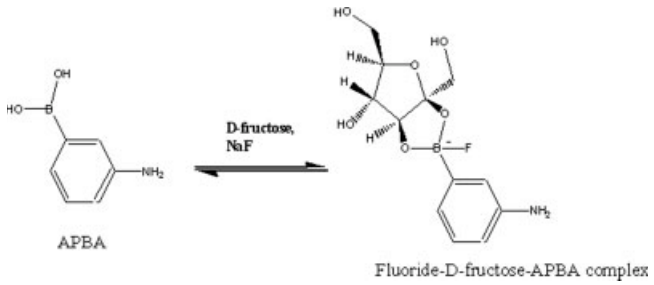

Scheme 1 Formation of APBA-fluoride-D-fructose complex in the absence of SiO_2 nanoparticles.

nanoparticles. While pristine SiO_2 nanoparticles [Fig. 1(c)] are spherical, a core-shell type morphology can be seen for SiO_2/PAPBA-NC**1** [Fig. 1(a)]. SiO_2 nanoparticles have smooth outer surfaces and the average diameter of particles is ~10 nm [Fig. 1(c)]. On the other hand, SiO_2/PAPBA-NC**1** has smooth and uniform coating of PAPBA (~10 nm) over the SiO_2 nanoparticles (~10 nm) and the average size of SiO_2/PAPBA-NC**1** is ~20 nm. However, SiO_2 nanoparticles are submerged in the mass of PAPBA for SiO_2/PAPBA-NC**2** [Fig. 1(b)].

The formation of core–shell morphology for SiO_2/PAPBA-NC**1** is explained as follows. There can be chemical interactions between boronic acid or boronate groups and anions (hard bases) like F^- to result adducts. While forming such adducts, sp^2 hybridization in form changes to sp^3 hybridization.[59–61] Further, boronic acids have tendency to form complexation (tetrahedral boronate esters) with compounds having hydroxyl groups or diol or polyol moieties at pH = 7 in the presence of F^- ions. In the present study, we envisage binding of SiO_2 nanoparticles to APBA via complexation (as described in Schemes 1 and 2). APBA molecules that are bound to SiO_2 nanoparticles undergo polymerization to result core-shell SiO_2/

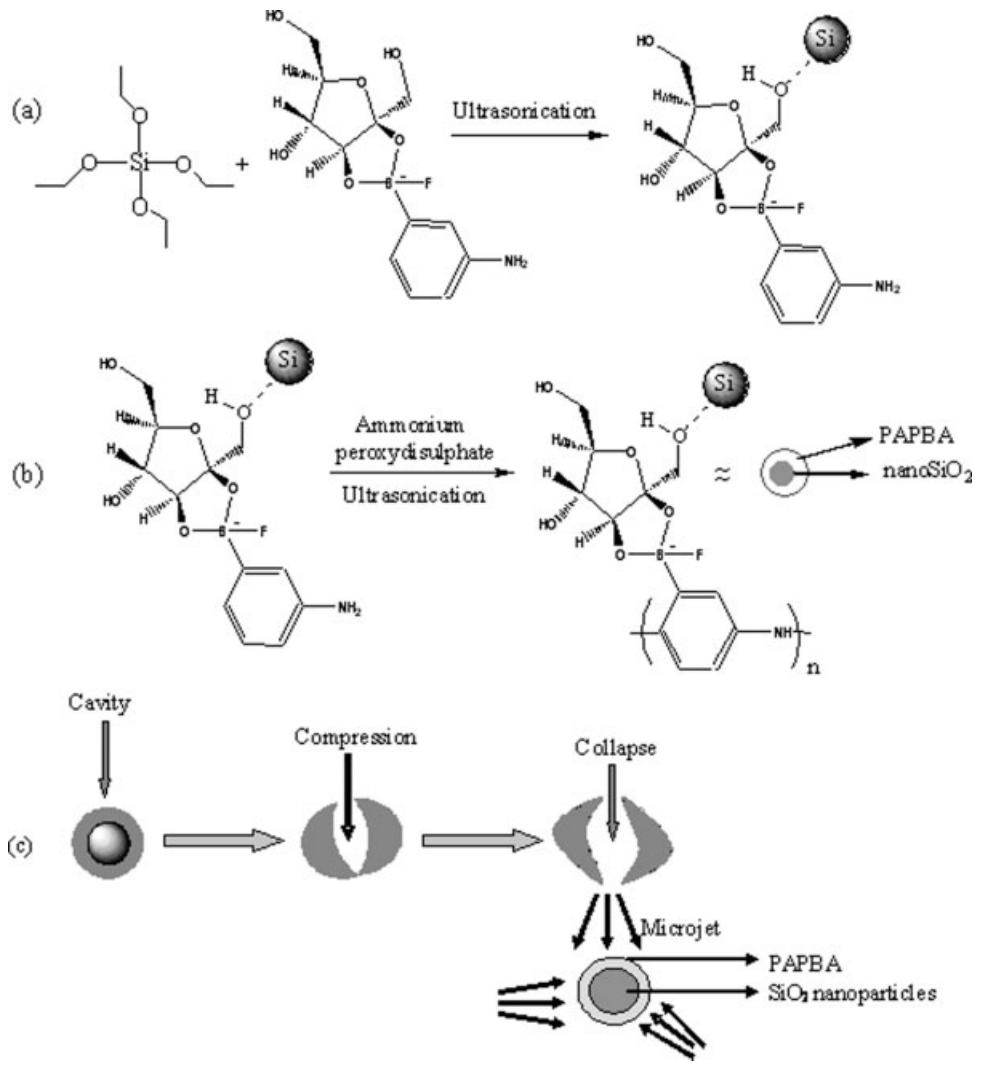

Scheme 2 (a) Typical representation showing the anchoring of APBA-fluoride-D-fructose complex onto SiO_2 nanoparticles, (b) polymerization of APBA-F^--D-fructose complex in the presence of SiO_2 nanoparticles, and (c) formation process of core-shell SiO_2/PAPBA-NC1 via ultrasonication.

PAPBA type nanocomposite. On the other hand, there is no core-shell morphology for SiO_2/PAPBA-NC**2** [Fig. 1(b)]. Hence, it is concluded that core-shell type SiO_2/PAPBA nanocomposite resulted only in the presence of F^- ions. Now, the role of ultrasonication on the composite formation is explained. Under ultrasonication the SiO_2 nanoparticles are dispersed and present as individual nanoparticles. The SiO_2 nanoparticles form complexes with APBA in the presence of F^- ions and D-fructose (Schemes 1 and 2). Polymerization of APBA that is complexed to SiO_2 nanoparticles, a core-shell type nanocomposite, SiO_2/PAPBA-NC**1** is resulted. To ascertain the influence of ultrasonication on the morphology of SiO_2/PAPBA-NC1, the nanocomposite SiO_2/PAPBA was prepared under similar conditions but in the absence of ultrasonication (polymerization was performed with conventional stirring). SiO_2/PAPBA nanocomposite prepared in the absence of ultrasonication was present as aggregates [Fig. 1(d)]. The difference in the morphology of the composites [Fig. 1(a,c, and d)] reveals that core-shell composite [Fig. 1(a)] was obtained when polymerization of APBA was carried out in the combined presence of F^- ions and D-fructose under ultrasonication. With other conditions, SiO_2 nanoparticles were entrapped into PAPBA.

Ultrasonic irradiation in reaction system induces transient cavitations: the formation, growth, and implosive collapse of bubbles.[15] During the collapse of the bubble in the vicinity of SiO_2 nanoparticles suspended in reaction solution, a high-speed microjet and intense shock-waves with high pressure are generated at their liquid–solid (SiO_2) interface. As a result, effective mass transfer at the interface can happen that could increase the reaction activity.[16] Hence, it can be expected that such speed microjets with high pressure shock waves would influence the mass transport of polymer to the overall surface of the SiO_2 nanoparticles. As a result, a precise coating of PAPBA (shell) on the SiO_2 (core) would be achieved in the presence of F^- and D-fructose under ultrasonication [Scheme 2(c) and Fig. 1(a)]. Such core-shell morphology was not obtained when composite prepared in the presence of conventional stirring. Probably in the presence of ultrasonication high intense ultrasonic waves could push the silica nanoparticles into interior part of polymer. Also, in the presence of ultrasonication, the time of polymerization is minimum. On the other hand, conventional stirring leads to aggregation of composite particles as shown in Figure 1(d). The composites prepared in the presence of conventional stirring method has aggregated morphology as reported earlier.[62,63] Interestingly, SiO_2/PAPBA-NC**1** showed difference in electrical properties, structural characteristics, and thermal behavior in comparison to the SiO_2/PAPBA-NC**2**. Results from FTIR spectroscopy, UV-visible spectroscopy, XRD analysis, and thermogravimetric analysis reveal the differences in the structural, optical, morphological, and thermal characteristics between SiO_2/PAPBA-NC**1** and SiO_2/PAPBA-NC**2**.

Electronic states of SiO_2/PAPBA nanocomposites

Figure 2 presents the UV-visible spectra of SiO_2/PAPBA-NC**1** and SiO_2/PAPBA-NC**2**. Clearly, there are differences in the electronic states of PAPBA in these composites. The UV-visible spectrum of SiO_2/PAPBA-NC**1** [Fig. 2(a)] shows two bands one around 360 nm and an another around 560 nm, while the spectrum of SiO_2/PAPBA-NC**2** [Fig. 2(b)] has a broad band around 420 nm. The band characteristics in the UV-visible spectrum of SiO_2/PAPBA-NC**1** correspond to emeraldine salt form of unsubstituted PANI.[64] In the spectrum of SiO_2/PAPBA-NC**1**, the absorption band at 360 nm is assigned to the π–π^* transition, which is related to the extent of conjugation length, and the band at 560 nm is assigned to the exciton transition caused by interchain or intrachain charge transfer. Exciton transition band is absent and π–π^* transition band appeared at higher wavelength (420 nm) in the spectra of SiO_2/PAPBA-NC**2** is probably due to absence of anionic boronic ester complex structure. The presence of π–π^* and exciton transition bands in SiO_2/PAPBA-NC**1** suggests that PAPBA exists in a self-doped state. The self-doping in PAPBA arises from the formation of tetrahedral boronate complex in the presence of D-fructose and fluoride (Schemes 1 and 3). We, therefore envisage that PAPBA in SiO_2/PAPBA-NC**1** exists in the emeraldine salt form as a result of self-doping (Scheme 3). It is important to note that the self-doping of PAPBA in SiO_2/PAPBA-NC**1** is quite different from the generally reported self-doping for PANI derivatives, like

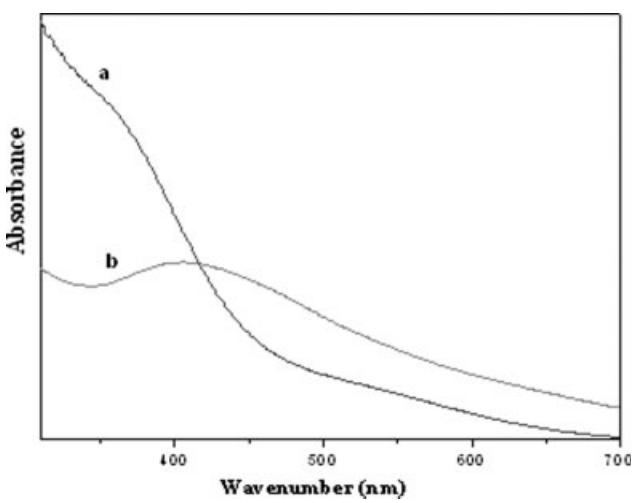

Figure 2 UV-visible spectra of (a) SiO_2/PAPBA-NC**1** and (b) SiO_2/PAPBA-NC**2**.

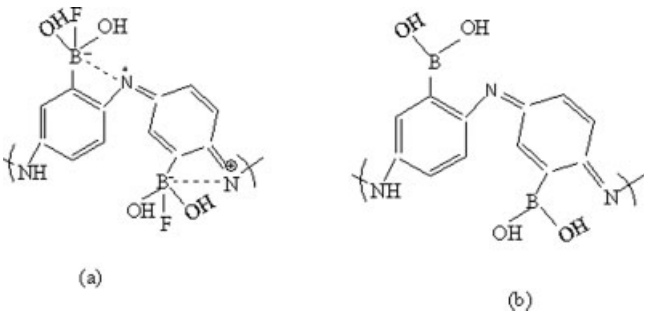

Scheme 3 (a) Structure of emeraldine salt (self-doped) form of PAPBA in SiO_2/PAPBA-NC**1** and (b) emeraldine form in PAPBA in SiO_2/PAPBA-NC**2**.

sulfonated PANI. In the sulfonated PANIs, the sulfonate groups induce doping in PANI chains. However, in the present case, the negative charge induced in boron atom induces doping [Scheme 3(a)]. The electronic bands of PAPBA units in SiO_2/PAPBA-NC**2** are similar to simple PANI. Hence, we have observed distinctly different electronic states for PAPBA in SiO_2/PAPBA-NC**1** and SiO_2/PAPBA-NC**2**.

Structural characteristics of SiO_2/PAPBA nanocomposites

FTIR spectra (Fig. 3) of SiO_2/PAPBA-NC**1** and SiO_2/PAPBA-NC**2** provide evidences for the differences in structural characteristics of PAPBA in the composites. FTIR spectrum of SiO_2/PAPBA-NC**1** [Fig. 3(a)] shows few main bands that are characteristics of SiO_2 nanoparticles (790, 960, and 1100 cm^{-1}) and PAPBA ($\sim$ 1630 and $\sim$ 1510 cm^{-1}). The bands around $\sim$ 1630 and $\sim$ 1510 cm^{-1} correspond to quinoid and benzenoid stretching units of PAPBA, respectively.[65,66] There are distinct differences in the band characteristics between SiO_2/PAPBA-NC**1** and SiO_2/PAPBA-NC**2**. FTIR spectrum of SiO_2/PAPBA-NC**1** [Fig. 3(a)] shows additional bands, $\sim$ 1340, $\sim$ 1060, and $\sim$ 880 cm^{-1} corresponding to asymmetric B—O stretching, C—O stretching modes in fructose units, B—F stretching, respectively. These bands indicate that SiO_2/PAPBA-NC**1** has boronate ester linkages with associated B—F groups as suggested in the Schemes 1 and 2. However, these bands are all not present in SiO_2/PAPBA-NC**2** and signify the absence of binding between boronate groups and SiO_2 nanoparticles. Also, the boronate ester formation through binding SiO_2 nanoparticles to boronate groups in PAPBA in SiO_2/PAPBA-NC**1** is the reason for inducing doping in the units of PAPBA. This was evident from a comparison of intensities of bands of quinoid (1630 cm^{-1}) and benzenoid (1510 cm^{-1}) C—N stretching bands. A ratio of 1.5 was noticed for SiO_2/PAPBA-NC**1**. This suggests that imine units are more than amine units in PAPBA, probably due to self-doping.

Thermal properties of SiO_2/PAPBA-NC nanocomposites

Figure 4 displays the thermogram of the nanocomposites, SiO_2/PAPBA-NC**1** and SiO_2/PAPBA-NC**2** and pristine SiO_2 nanoparticles. Thermograms of nanocomposites, SiO_2/PAPBA-NC**1** and SiO_2/PAPBA-NC**2**, show degradation characteristics of the backbone units of PAPBA. Interestingly, PAPBA units in those composites degrade at different temperatures. The degradation of PAPBA units in SiO_2/PAPBA-NC**1** starts at a higher temperature ($\sim$ 350°C) in the comparison with PAPBA units in SiO_2/PAPBA-NC**2** ($\sim$ 310°C). The binding of boronate groups to SiO_2 nanoparticles and self-doping in PAPBA as witnessed by FTIR spectroscopy [Fig. 3(a)] may be the reason for the increased thermal stability of PAPBA units in SiO_2/PAPBA-NC**1**.

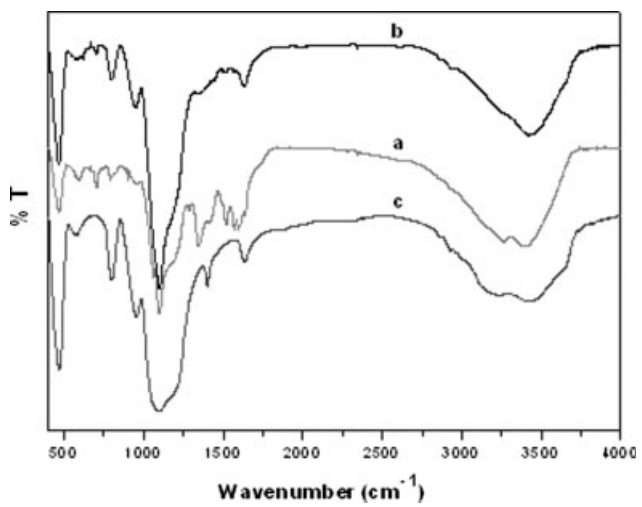

Figure 3 FTIR spectra of (a) SiO_2/PAPBA-NC**1**, (b) SiO_2/PAPBA-NC**2**, and (c) nano SiO_2 particles.

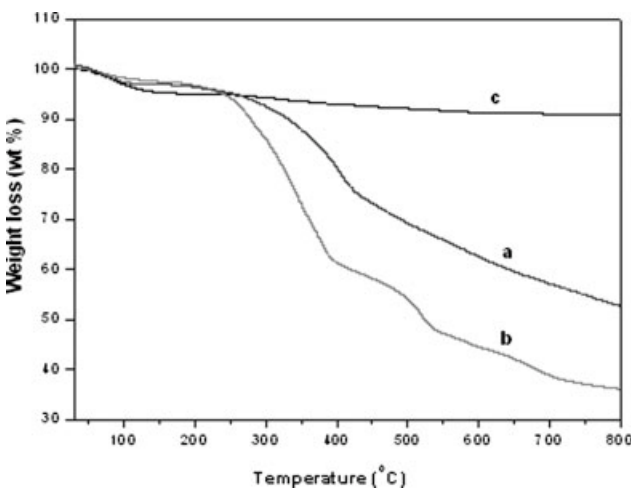

Figure 4 Thermogram of (a) SiO_2/PAPBA-NC**1**, (b) SiO_2/PAPBA-NC**2**, and (c) nanoSiO_2 particles.

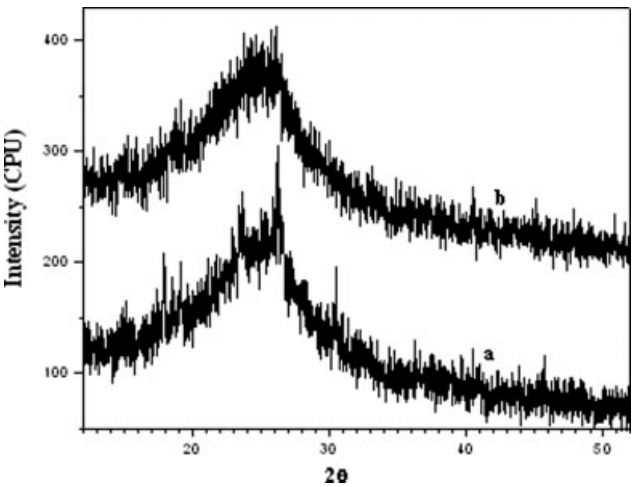

Figure 5 X-ray diffraction of (a) SiO_2/PAPBA-NC**1** and (b) SiO_2/PAPBA-NC**2**.

XRD analysis

Figure 5 shows the XRD patterns of SiO_2/PAPBA-NC**1** and SiO_2/PAPBA-NC**2**. The XRD patterns of SiO_2/PAPBA-NC**1** [Fig. 5(a)] show additional peaks around 23.5°, 26°, 31°, and 48° and inform the probable induced ordering in the composite. This may be due to the binding of boronate groups to SiO_2 as evidenced from FTIR spectroscopy (Fig. 3).

Conductivity

The conductivity of SiO_2/PAPBA-NC1 and SiO_2/PAPBA-NC2 are 0.21 and 4.6×10^{-3} S/cm, respectively. Conductivity of SiO_2/PAPBA composite prepared in the presence of conventional stirring was 5.3×10^{-2} S/cm. It reveals that composite prepared under ultrasonication contributes to the increase in conductivity in comparison with the composite prepared with conventional stirring. The higher conductivity of SiO_2/PAPBA-NC1 over SiO_2/PAPBA-NC2 is attributed to (i) well dispersed SiO_2 nanoparticles (core) in the polymer (shell) favors electronic transport, (ii) enhancement of thermal stability,[67] (iii) better morphological structure, and (iv) self-doped nature of polymer in the composite as observed from TEM, TGA, and FTIR results.

CONCLUSIONS

Core-shell type SiO_2/poly(amonophenylboronic acid) nanocomposite was formed due to interactions between functional groups (boronic acid) in the conducting polymer and hydroxyl groups in SiO_2 nanoparticles. Anchoring of conducting polymers having functional groups over the inorganic nanoparticles influence the electronic and thermal property of the resulting composites. Composite prepared in the presence of NaF and D-fructose via ultrasonication has core–shell morphology and has few interesting characteristics than the nanocomposite prepared conventional stirring method.

The authors acknowledge Kyungpook National University Center for Scientific Instruments.

References

1. Gratzel, M. Nature 2001, 414, 338.
2. Zeng, H.; Li, J.; Liu, J. P.; Wang, Z. L.; Sun, S. Nature 2002, 420, 395.
3. Huang, J.; Virji, S.; Weiller, B. H.; Kaner, R. B. J Am Chem Soc 2003, 125, 314.
4. Langer, R.; Tirrels, D. A. Nature 2004, 428, 487.
5. Besteman, K.; Lee, J.; Wiertz, F. G. M.; Heering, H. A.; Dekker, C. Nano Lett 2003, 3, 727.
6. Lim, J. H.; Mirkin, C. A. Adv Mater 2002, 16, 1474.
7. Ng, M. K.; Yu, L. P. Angew Chem Int Ed 2002, 41, 3598.
8. Demoustier, S. C.; Legras, R.; Jerome, R. Chem Eur J 2000, 6, 3089.
9. Ikegame, M.; Tajima, K.; Aida, T. Angew Chem Int Ed 2003, 42, 2204.
10. Jang, J.; Yoon, H. Chem Commun 2003, 720.
11. Hulvat, J. F.; Stupp, S. I. Adv Mater 2004, 16, 589.
12. Reddy, K. R.; Lee, K. P.; Gopalan, A. I.; Ali, M. S. Polym J 2006, 38, 349.
13. Brustolin, F.; Goldoni, F.; Meijer, E. W.; Sommerdijk, N. A. J. M. Macromolecules 2002, 35, 1054.
14. Goto, H.; Yashima, E. J Am Chem Soc 2002, 124, 7943.
15. Flint, E. B.; Suslick, K. S. Science 1991, 253, 1397.
16. Suslick, K. S. J Am Chem Soc 1996, 118, 11960.
17. Fujimoto, T.; Terauchi, S.; Umehara, H.; Kojima, I.; Henderson, W. Chem Mater 2001, 13, 1057.
18. Li, Q.; Li, H.; Pol, V. G.; Bruckental, I.; Koltypin, Y.; Moreno, J. C.; Nowik, I.; Gedanken, A. New J Chem 2003, 27, 1194.
19. Hyeon, T.; Fang, M.; Suslick, K. S. J Am Chem Soc 1996, 118, 5492.
20. Srivastava, D. N.; Pol, V. G.; Palchik, O.; Zhang, L.; Yu, J. C.; Gedanken, A. Ultrason Sonochem 2005, 12, 205.
21. Wang, H.; Zhang, J. R.; Zhao, X. N.; Xu, X.; Zhu, J. J. Mater Lett 2002, 55, 253.
22. Levi, S. A.; Nitzan, Y.; Dror, R.; Gedanken, A. J Am Chem Soc 2003, 125, 15712.
23. Ding, T.; Zhang, J.; Hong, J.; Zhu, J.; Chen, H. J Cryst Growth 2004, 260, 527.
24. Qiu, L.; Pol, V. G.; Wei, Y.; Gedanken, A. New J Chem 2004, 28, 1056.
25. Suslick, K. S.; Choe, S. B.; Cichowals, A. A.; Grinstaff, M. W. Nature 1991, 353, 414.
26. Jeong, S. H.; Ko, J. H.; Park, J. B.; Park, W. J Am Chem Soc 2004, 126, 15982.
27. Yu, Y.; Ma, L. L.; Huang, W. Y.; Du, F. P.; Yu, J. C.; Yu, J. G.; Wang, J. B.; Wong, P. K. Carbon 2005, 43, 651.
28. Reddy, K. R.; Lee, K. P.; Gopalan, A. I.; Kim, M. S.; Ali, M. S.; Nho, Y. C. J Polym Sci Part A: Polym Chem 2006, 44, 3355.
29. Kumar, R. V.; Palchik, O.; Koltypin, Y.; Diamant, Y.; Gedanken, A. Ultrason Sonochem 2002, 9, 65.
30. Wang, J.; Yuan, H.; Wang, S.; Chen, Z. Ultrason Sonochem 2005, 12, 165.
31. Wang, Q.; Xia, H. S.; Zhang, C. H. J Appl Polym Sci 2001, 80, 1478.
32. Jing, X.; Wang, Y.; Wu, D.; She, L.; Guo, Y. J Polym Sci Part A: Polym Chem 2005, 98, 2149.

33. Nikitenko, S. I.; Yu, K.; Pickup, D. M.; Van-Eck, E. R. H.; Gedanken, A. Ultrason Sonochem 2003, 10, 11.
34. Bradley, M.; Grieser, F. J Colloid Interface Sci 2002, 251, 78.
35. Kumar, R. V.; Mastai, Y.; Gedanken, A. Ultrason Sonochem 2000, 12, 3892.
36. Kwon, J. Y.; Koo, Y. S.; Kim, H. D. J Appl Polym Sci 2004, 93, 700.
37. Showkat, A. M.; Lee, K. P.; Gopalan, A. J. Appl Polym Sci, to appear.
38. Skotheim, J. R.; Elsenbaumer, R. L.; Reynolds, J. R. Handbook of Conducting Polymers, 2nd ed.; Marcel Dekker: New York, 1998.
39. Ghosh, P.; Siddhanta, S. K.; Haque, S. R.; Chakrabariti, A. Synth Met 2001, 123, 83.
40. Chem, S. A.; Hwang, G. W. J Am Chem Soc 1994, 116, 7939.
41. Pringsheim, E.; Zimin, D.; Wolfbeis, O. S. Adv Mater 2001, 13, 819.
42. Nicolas, M.; Fabre, M.; Marchand, G.; Simonet, J. J Org Chem 2000, 9, 1703.
43. Wei, X. L.; Wang, Y. A.; Long, S. M.; Bobeczko, C.; Epstein, A. J. J Am Chem Soc 1996, 118, 2545.
44. Liu, S.; Miller, B.; Chen, A. Electrochem Commun 2005, 7, 1232.
45. Ma, Y.; Li, N.; Yang, C.; Yang, X. Colloids Surf A 2005, 269, 1.
46. John, R.; Chou, T. C. Biosens Bioelectron 2006, 22, 329.
47. Fabre, B.; Taillebois, L. Chem Commun 2003, 2982.
48. Deore, B. A.; Hachey, S.; Freund, M. S. Chem Mater 2004, 16, 1427.
49. Ma, Y.; Ali, S. R.; Dodoo, A. S.; He, H. J Phys Chem B 2006, 110, 16359.
50. Garotenuto, G.; Nicolais, L.; Mortorana, B.; Perlo, P. Metal-Polymer Nancomposites; Wiley: New York, 2004.
51. Anjali, A. A.; Bhagwat, S. V.; Katre P. P. Sen Actuators B 2006, 114, 263.
52. Kageyama, K.; Tamazawa, J.; Aida, T. Science 1999, 285, 2113.
53. Caruso, F.; Mohwald, H. Science 1998, 282, 1111.
54. Tong, X.; Tang, T.; Feng, Z.; Huang, B. J Appl Polym Sci 2002, 86, 3532.
55. Ahn, S. H.; Kim, S. H.; Lee, S. G. J Appl Polym Sci 2004, 94, 812.
56. Zhang, J.; Zhu, B. K.; Chu, H. J.; Xu, Y. Y. J Appl Polym Sci 2005, 97, 20.
57. Das, A.; De, D.; Naskar, N.; Debnath, S. C. J Appl Polym Sci 2006, 99, 1132.
58. La, H. S.; Park, K. S.; Nahma, K. S.; Jeong, K. K.; Lee, Y. S. Colloids Surf A 2006, 272, 22.
59. Cooper, C. R. Chem Commun 1998, 13, 1365.
60. Dusemund, C.; Sandanayake, K. R. A. S.; Shinkai, S. J Chem Soc Chem Commun 1995, 3, 407.
61. Yamamoto, H.; Ori, A.; Ueda, K.; Dusemund, C.; Shikai, S. Chem Commun 1996, 3, 407.
62. Xia, H.; Wang, Q. Chem Mater 2002, 14, 2158.
63. Jing, X.; Wang, Y.; Wu, D.; Qiang, J. Ultrason Sonochem 2007, 14, 75.
64. Stilwell, D. A.; Park, S. M. J Electrochem Soc 1989, 136, 427.
65. Colthup, N. B.; Daly, L. H.; Wiberley, S. E. Introduction to Infrared and Raman Spectroscopy; Academic Press: New York, 1975.
66. Epstein, A. J.; Mcall, R. P.; Ginder, J. M.; MacDiarmid, A. G. Spectroscopy Advanced Materials; Wiley: New York, 1991.
67. Wang, Y.; Rubner, M. F. Synth Met 1992, 47, 255.